



DØnote 5355-CONF

## Measurement of the $t\bar{t}$ pair production cross section in $p\bar{p}$ collisions at $\sqrt{s} = 1.96$ TeV in the lepton+jets final state using lifetime tagging on 900 pb<sup>-1</sup> of DØ data

The DØ Collaboration  
URL: <http://www-d0.fnal.gov>  
(Dated: March 10, 2007)

We present a preliminary measurement of the  $t\bar{t}$  production cross-section in  $p\bar{p}$  collisions at  $\sqrt{s} = 1.96$  TeV, based on the application of a neural network  $b$ -tagging algorithm to about 900 pb<sup>-1</sup> of DØ data in the  $e$ +jets and  $\mu$ +jets channels. We measure

$$\begin{aligned} e + \text{jets} : \quad \sigma_{p\bar{p} \rightarrow t\bar{t}+X} &= 7.4 \pm 0.7(\text{stat}) \begin{matrix} +0.8 \\ -1.0 \end{matrix}(\text{syst}) \pm 0.4(\text{lumi}) \text{ pb} \\ \mu + \text{jets} : \quad \sigma_{p\bar{p} \rightarrow t\bar{t}+X} &= 9.5 \pm 0.9(\text{stat}) \begin{matrix} +1.1 \\ -1.3 \end{matrix}(\text{syst}) \pm 0.6(\text{lumi}) \text{ pb} \\ \ell + \text{jets} : \quad \sigma_{p\bar{p} \rightarrow t\bar{t}+X} &= 8.3 \begin{matrix} +0.6 \\ -0.5 \end{matrix}(\text{stat}) \begin{matrix} +0.9 \\ -1.0 \end{matrix}(\text{syst}) \pm 0.5(\text{lumi}) \text{ pb} \end{aligned}$$

*Preliminary result for spring conferences 2007*

## I. INTRODUCTION

In  $p\bar{p}$  collisions at Tevatron energies, the top quark is dominantly produced in top-antitop quark pairs via the strong interaction. The cross section for this process can be calculated to 15% precision [1, 2]. With the large data samples from Run II of the Tevatron, experimental precision approaches the same level thus providing a sensitive test of the QCD calculations. Deviations from the predicted value could indicate the contribution of non-standard processes to top quark production.

In the standard model, the top quark decays almost always to a  $W$  boson and a  $b$  quark. The possible final states are then determined by the decay modes of the two  $W$  bosons. In this analysis events in which one  $W$  boson decays to leptons ( $e$  or  $\mu$ , including  $e$  or  $\mu$  from  $\tau$  decays) and the other  $W$  boson decays to hadrons are considered. The final state therefore consists of one isolated, high  $p_T$  lepton, missing transverse momentum ( $\cancel{E}_T$ ) from the undetected neutrino, and a number of jets. This channel is called the lepton+jets channel.

There are two major sources of background that contribute to the lepton+jets data samples. The dominant background is production of  $W$  bosons in association with jets with the  $W$  boson decaying leptonically ( $W$ +jets). This process produces the same final state as  $t\bar{t}$  production. The second major background is instrumental, originating from multijet events in which one of the jets is misidentified as an isolated electron or in which a muon appears isolated because the associated jet was not reconstructed.

The  $b$ -flavored hadrons from the hadronization of the  $b$  quarks from top quark decay have a relatively long lifetime. They travel far enough that their decay vertex can be resolved from the primary event vertex at which the  $p\bar{p}$  collision occurred. Tagging  $b$ -jets using the long lifetime of  $b$ -flavored hadrons is called lifetime tagging and provides a powerful tool to separate the  $t\bar{t}$  signal from background.

Here we present a preliminary measurement of the  $t\bar{t}$  production cross section in the lepton+jets channel using lifetime tagging based on a data set of about  $900 \text{ pb}^{-1}$  collected by the D0 experiment.

## II. THE D0 DETECTOR

The D0 detector is a multipurpose collider detector [3]. The central tracker employs silicon microstrips close to the beam and concentric cylinders covered with scintillating fibers in a 2 T magnetic field parallel to the beam axis. The liquid-argon/uranium calorimeter is divided into a central section covering  $|\eta| \leq 1.1$  and two endcap calorimeters extending coverage to  $|\eta| \leq 4.2$  [4], where  $\eta = -\ln[\tan(\theta/2)]$  and  $\theta$  is the polar angle with respect to the proton beam direction. The muon spectrometer consists of a layer of drift chambers and scintillation counters between the calorimeter and 1.8 T toroidal magnets, followed by two similar layers outside the toroids.

## III. DATA SAMPLE

The data were collected between August 2002 and December 2005. For the  $e$ +jets channel a total of  $913 \text{ pb}^{-1}$  were accumulated using triggers that require one electron with  $p_T > 15 \text{ GeV}$  and at least one jet with  $p_T$  thresholds between 15 and 30 GeV, depending on running period. For the  $\mu$ +jets channel  $871 \text{ pb}^{-1}$  were accumulated requiring a muon and at least one jet with  $p_T$  thresholds between 20 and 35 GeV in the trigger.

## IV. MONTE CARLO SIMULATION

The signal is modeled by  $t\bar{t}$  events generated with ALPGEN[5], assuming  $m_{top} = 175 \text{ GeV}$ . The dominant  $W$ +jets background is modeled by  $Wb\bar{b} + Wc\bar{c} + Wj\bar{j}$  events generated using ALPGEN. The process  $W + c$  is generated along with the  $W$ +light quark jets. We use ALPGEN to generate events with additional partons at leading order, e.g.  $W+1, 2, 3, 4,$  and  $5$  or more partons. For all these samples we use PYTHIA[6] to fragment and hadronize quarks and gluons. We then employ a jet-matching algorithm, following the MLM prescription [7], that ensures that there is no double counting due to the parton showering in PYTHIA.

Single top event samples were generated by the CompHEP-SingleTop[8] Monte Carlo event generator, assuming  $m_{top} = 175 \text{ GeV}$ . SINGLETOP produces events whose kinematic distributions match those from NLO calculations. PYTHIA was used to add the underlying event and initial- and final-state radiation.

TAUOLA [9] was used to decay tau leptons, and EVTGEN [10] to decay  $b$  hadrons.

The D0 detector is simulated using the GEANT[11] program and all events are reconstructed with the standard D0 reconstruction program.

## V. EVENT RECONSTRUCTION

The D0 reconstruction program defines the following objects as a basis for event selection.

The primary event vertex defines the position of the hard  $p\bar{p}$  interaction in the detector and is the reference point for the calculation of kinematic variables, such as transverse momenta.

Electrons are reconstructed as clusters of energy depositions with at least 90% of their energy in the electromagnetic section of the calorimeter. The profile of the clusters must be consistent with the electromagnetic shower profile predicted by a simulation. The cluster must be isolated from other energy deposits in the calorimeter. The fraction of energy in an annular isolation cone of radius  $0.2 < R = \sqrt{\Delta\phi^2 + \Delta\eta^2} < 0.4$  must be less than 15% of the energy in the core cone of radius  $R < 0.2$ . Every electron must be matched in  $\eta$  and  $\phi$  with a track with  $p_T > 5$  GeV reconstructed in the central tracker.

Muons are reconstructed primarily as tracks in the muon spectrometer. We accept muons with  $|\eta| < 2$ . We reject cosmic rays by requiring the time of hits in the muon scintillation counters to be within 10 ns of the beam crossing time. The track reconstructed in the muon system must match a track reconstructed in the central tracker with a distance of closest approach to the beam line in the transverse plane  $< 200 \mu\text{m}$  if it has hits in the silicon tracker or  $< 2$  mm if it does not. Muons must be separated from jets by  $R > 0.5$ , the energy measured in the calorimeter in an annular cone of radius  $0.1 < R < 0.4$  around the muon direction must be less than 8% of the muon  $p_T$  and the momenta of all tracks in a cone of radius  $R < 0.5$  around the muon direction, except the track matched to the muon, must add up to less than 6% of the muon  $p_T$ .

Jets are reconstructed from energy deposits in the calorimeter using the Run 2 cone algorithm [12] with a cone of  $R < 0.5$ . To eliminate jets seeded by calorimeter noise, the following quality criteria are applied: The energy in the electromagnetic section of the calorimeter must be greater than 5% and less than 95% of the total jet energy. The energy in the coarse hadronic calorimeter must be less than 40% of the total jet energy. The ratio of the highest to the second highest cell in transverse energy must be less than 10. No tower may contain more than 90% of the jet energy. The reconstructed jet must also be consistent with the information from the level 1 calorimeter trigger. All jet energies are corrected to the particle level.

Jets can be tagged as originating from the fragmentation of a  $b$  quark. The algorithm uses a neural network to combine the outputs of several  $b$ -tagging algorithms. The seven input variables are a combination of the track impact parameter significances, the probability that all the tracks originated from the primary vertex, the number of secondary vertices in a jet, and for secondary vertices the decay length significance, goodness of fit of the vertex, invariant mass of all tracks, and the number of tracks associated with the vertex. For the cut on the neural network discriminant that we use the  $b$ -tagging efficiency is approximately 54% at a fake tag rate just below 1% for taggable jets. Taggable jets have at least two tracks with at least one hit in the silicon microstrip tracker in a cone of  $R < 0.5$ , matched to the jet. About 75% of all jets are taggable.

Neutrinos carry away transverse momentum that can be inferred using momentum conservation in the transverse plane. We compute the missing transverse momentum by adding vectorially the transverse energies measured in all cells of the electromagnetic and fine hadronic calorimeters. Cells in the coarse hadronic calorimeter are added only if they are part of a good jet. This raw quantity is then corrected for the energy corrections applied to the reconstructed objects and for the momentum of all muons in the event, corrected for their energy loss in the calorimeter.

## VI. EVENT SELECTION

The signature of the lepton+jets channel is one isolated lepton with high transverse momentum, large  $\cancel{E}_T$  due to the undetected neutrino and four or more jets with high transverse momentum, two of which originate from the fragmentation of  $b$ -quarks. The selection is designed to define a data sample enriched in  $W$ +jets and  $t\bar{t}$  events. To ensure that there is no overlap between the two lepton+jets channels and dilepton channels, events with a second lepton with high transverse momentum are explicitly vetoed.

The following requirements are imposed to select the data sample for the  $e$ +jets channel:

- primary vertex with  $|z| \leq 60$  cm and at least 3 tracks;
- one electron with  $p_T > 20$  GeV and  $|\eta| < 1.1$  and originating from the primary vertex;
- no second electron with  $p_T > 15$  GeV ;
- no isolated muon with  $p_T > 15$  GeV;
- at least one jet with  $p_T > 20$  GeV and  $|\eta| < 2.5$ ;

- $\cancel{E}_T > 20$  GeV and  $\Delta\phi(e, \cancel{E}_T) > 0.7 \cdot \pi - 0.045 \cdot \cancel{E}_T$  (Fig. 1).

For the  $\mu$ +jets channel the selection requirements are as follows:

- primary vertex with  $|z| \leq 60$  cm and at least 3 tracks;
- one muon with  $p_T > 20$  GeV and originating from the primary vertex;
- invariant mass of the selected muon and any second muon candidate  $m_{\mu\mu} < 70$  GeV or  $m_{\mu\mu} > 110$  GeV to reject  $Z(\rightarrow \mu\mu)$ +jet events;
- no second muon with  $p_T > 15$  GeV;
- no isolated electron with  $p_T > 15$  GeV;
- at least one jet with  $p_T > 20$  GeV and  $|\eta| < 2.5$ ;
- $\cancel{E}_T > 20$  GeV and  $\Delta\phi(e, \cancel{E}_T) > 0.48 \cdot \pi - 0.033 \cdot \cancel{E}_T$  (Fig. 1)
- transverse mass  $> 30$  GeV.

We use events with one or two jets as background dominated control samples and events with three or more jets to measure the  $t\bar{t}$  cross section. We will refer to a tight selection for which the primary lepton in the above selections is required to be isolated and to a loose selection for which this isolation requirement is not imposed.

Table 1 lists the efficiencies for the tight selection and the numbers of events selected in the data. The efficiencies for the selection of  $t\bar{t}$  events are measured in  $t\bar{t}$  Monte Carlo simulation with respect to  $t\bar{t} \rightarrow \ell\nu q\bar{q}'b\bar{b}$ , where  $\ell$  can be an electron or muon from the decay of a  $W$  boson, including  $W \rightarrow \tau\nu$  decays. The total efficiencies are corrected for trigger efficiencies and for differences between the Monte Carlo simulation and the collider data by applying scale factors.

TABLE 1: Summary of the selection efficiencies and data/MC correction factors in %, using statistical uncertainties only.

	$e + 3$ jets	$e + \geq 4$ jets	$\mu + 3$ jets	$\mu + \geq 4$ jets
selection efficiency	$14.68 \pm 0.07$	$14.08 \pm 0.07$	$11.96 \pm 0.07$	$12.80 \pm 0.07$
trigger efficiency	$96.43 \pm 0.02$	$96.68 \pm 0.01$	$86.88 \pm 0.07$	$87.33 \pm 0.07$
data/MC correction	$87.82 \pm 0.03$	$87.80 \pm 0.03$	$89.95 \pm 0.06$	$89.97 \pm 0.06$
total efficiency	$12.08 \pm 0.09$	$11.62 \pm 0.08$	$9.10 \pm 0.07$	$9.80 \pm 0.07$
number of events selected	1541	348	1342	360

## VII. BACKGROUND NORMALIZATION

The selected event sample consists of events from  $W$ +jets production (the dominant contribution), multijet events, events from diboson production, and  $t\bar{t}$  events. We find that the contribution from diboson production is very small (less than an event in each the  $e$ +jets and  $\mu$ +jets channels) and we therefore neglect them in the following.

In multijet production, events with a misidentified lepton,  $\cancel{E}_T$  can arise from fluctuations and mismeasurements of the jet or lepton momenta. In this case  $\cancel{E}_T$  tends to be collinear with a reconstructed object (lepton or jet) in the event. In our event selection, we suppress these background events by applying a cut on  $\cancel{E}_T$  and the azimuthal separation between  $\cancel{E}_T$  and the lepton without losing much signal. The effect of this cut on a background enhanced sample is shown in Figure 1.

We determine the remaining instrumental background contamination directly from the data by using the loose selection. Events with misidentified leptons and events with a prompt high- $p_T$  lepton pass the tight selection cut with different efficiencies. Signal events pass the tight selection cuts with efficiencies of

$$\begin{aligned} \varepsilon &= 83.8 \pm 1.0(stat) \pm 2.0(syst) \% \text{ for } e\text{-jet events,} \\ \varepsilon &= 84.9 \pm 1.0(stat) \pm 1.7(syst) \% \text{ for } \mu\text{-jet events,} \end{aligned}$$

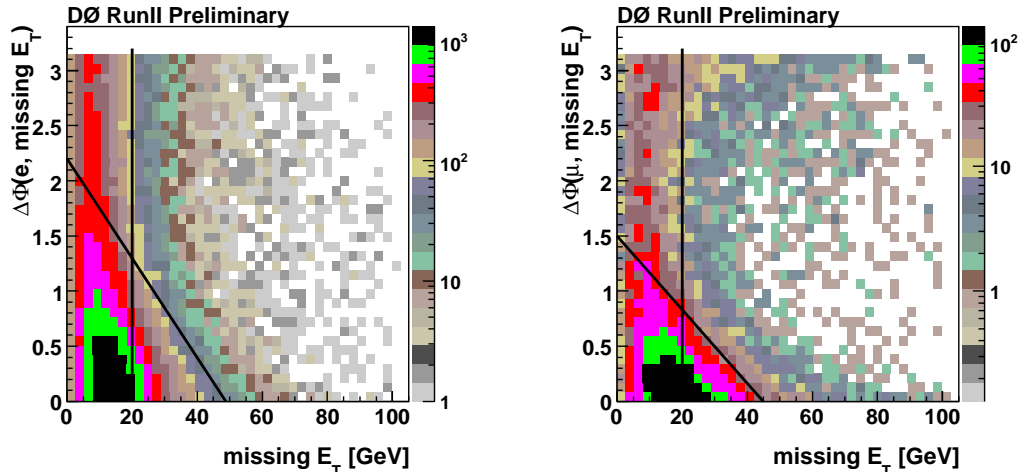


FIG. 1: Azimuthal separation between the isolated lepton and  $\cancel{E}_T$  for  $e$ +jets events (left) and  $\mu$ +jets events (right). The selection was relaxed to include events with at least two jets in order to increase the number of events. To show a background dominated sample, lepton quality cuts have been inverted. Similar distributions are observed for other jet multiplicities.

as determined from simulated  $W$ +jets and  $t\bar{t}$  events, corrected for data-MC differences. The probability that a misidentified lepton in the loose sample also passes the tight selection is

$$\begin{aligned}\varepsilon' &= 18 \pm 1(\text{stat}) \pm 3(\text{syst}) \% \text{ for } e\text{-jet events,} \\ \varepsilon' &= 24 \pm 1(\text{stat}) \pm 3(\text{syst}) \% \text{ for } \mu\text{-jet events,}\end{aligned}$$

as determined from a data sample that is dominated by misidentified leptons. We obtain this sample by using the loose selection but requiring low  $\cancel{E}_T$  to eliminate the  $W$  boson decays. We can relate the numbers of events with prompt leptons ( $N$ ) and misidentified leptons ( $N'$ ) in the loose sample to the observed total number of events in the loose sample ( $N_L$ ) and in the tight sample ( $N_T$ ). We get

$$\begin{aligned}N_L &= N + N' \\ N_T &= \varepsilon N + \varepsilon' N' .\end{aligned}$$

We solve this system of equations for  $N'$  and  $N$ . Table 2 lists the results. The product  $\varepsilon' N'$  gives us the number of events with misidentified leptons in the tight data sample.

The  $W$ +jets background is modelled by the Monte Carlo simulation. We find that we need to enhance the  $Wb\bar{b}$  and  $Wc\bar{c}$  contribution to the  $W$ +jets background by a factor  $1.5 \pm 0.45$  relative to the ALPGEN prediction to get the best agreement between background model and data. We normalize the total number of  $W$ +jets events to the number of events with prompt leptons in the tight data sample ( $\varepsilon N$ ), corrected for the small contribution expected from  $t\bar{t}$  events.

TABLE 2: Number of events in the loose and tight selected samples and the expected contribution from leptons from  $W$  boson decays and multijet background.

sample	$N_L$	$N_T$	$\varepsilon N$	$\varepsilon' N'$
$e + 3$ jets	3059	1541	1261	281
$e + \geq 4$ jets	680	348	287	61
$\mu + 3$ jets	1923	1342	1227	115
$\mu + \geq 4$ jets	500	360	334	26

In order to compare our background and signal model to the data we take the shape of the distributions of events with misidentified leptons from the data that pass the loose selection but not the tight selection. We find that in the  $\mu$ +jets channel this model does not agree perfectly with the data. We therefore apply an additional cut on the

transverse mass ( $m_T > 30$  GeV) to further reduce the contamination from misidentified leptons. After this cut we observe good agreement between data and model. Figure 2 shows the composition of the samples with four or more jets versus the transverse mass, computed from lepton  $p_T$  and  $\cancel{E}_T$ .

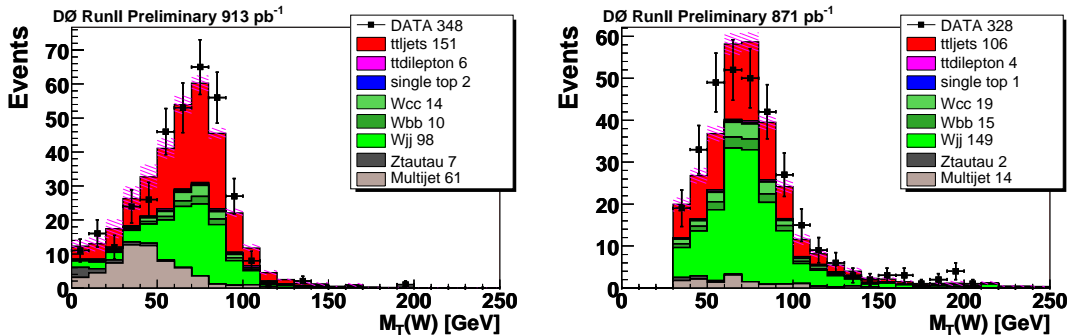


FIG. 2: Transverse mass distributions for the selected  $e$ +jets (left) and  $\mu$ +jets (right) sample with determined fractions of leptons from  $W$  boson decays and multijet background. The signal is broken down into  $t\bar{t} \rightarrow \ell$ +jets and  $t\bar{t} \rightarrow \ell\ell'$  events and the  $W$ +jets background is broken down into  $W + c\bar{c}$ ,  $W + b\bar{b}$ ,  $W + q\bar{q}$ . The hatched band indicates the uncertainties in the model.

### VIII. NUMBER OF $t\bar{t}$ EVENTS

The purpose of the event selection is to extract  $W \rightarrow \text{lepton} + \text{jets}$  events with maximum efficiency while rejecting multijet events. In order to enhance the  $t\bar{t}$  contribution in the data sample we require at least one of the jets to be tagged as a  $b$ -jet. We estimate the numbers of events from the  $W$ +jets background in the  $b$ -tagged event samples by weighting the  $W$ +jets events before tagging with their event-by-event tagging probability. The tagging probabilities for  $b$ -jets are measured using the Monte Carlo simulation and parametrized as a function of  $p_T$  and  $\eta$ . They are then multiplied by a data/MC scale factor, also parametrized in  $p_T$  and  $\eta$ , determined from data and Monte Carlo samples that were enriched in their  $b$ -jet content by requiring a muon in every event. The event tagging probability is then calculated from the tagging probabilities of all the jets in the event.

We determine the number of events with misidentified leptons by repeating the procedure described in section VII for the  $b$ -tagged samples.

We now determine the excess of events in the samples that pass the tight selection, have at least three jets and at least one  $b$ -tagged jet. Most of this excess originates from the decay  $t\bar{t} \rightarrow \ell\nu b q \bar{q}' \bar{b}$  but there is also a small contribution from  $t\bar{t} \rightarrow \ell^+ \nu b \ell'^- \bar{\nu}' \bar{b}$ . We consider both part of our signal. We measure the excess separately in eight different channels, defined by the two lepton flavors, the jet multiplicity (three and four or more jets) and the tag multiplicity (one and two or more tagged jets). Table 3 lists the event yields.

Figures 3- 5 show the predicted sample composition for the samples with exactly one tagged jet and with two or more tagged jets as a function of jet multiplicity.

Figure 6 shows comparisons of signal and background models with data in different kinematical variables for events with at least four jets of which at least one is  $b$ -tagged for the combined  $e$ +jets and  $\mu$ +jets samples.

### IX. CROSS SECTION DETERMINATION

The cross section is calculated by performing a maximum likelihood fit to the observed number of events in the eight different channels. The resulting cross sections are given for the electron and the muon channels separately and combined. The likelihood to observe  $N_i$  events for a cross section  $\sigma_{t\bar{t}}$  is proportional to:

$$\mathcal{L} = \prod_i \mathcal{P}(N_i, \mu_i(\sigma_{t\bar{t}})) \quad (1)$$

where  $i$  runs over all 8 channels when the total combined cross section is computed and  $\mathcal{P}(N; \mu)$  denotes the Poisson probability to observe  $N$  events when  $\mu$  events are expected. The expected number of events in each channel is the sum of the expected number of background events and the number of expected  $t\bar{t}$  events as a function of the  $t\bar{t}$  cross

TABLE 3: Expected event yields for signal (assuming  $\sigma_{t\bar{t}} = 6.8$  pb) and background and observed event yields. The uncertainties in the expected background events include the statistical uncertainty from the normalization to data and the dominant systematics from  $\varepsilon_{sig}$ ,  $\varepsilon_{QCD}$ , and the heavy flavor fraction in the  $W$ +jets background.

	$e+3$ jets	$e+\geq 4$ jets	$\mu+3$ jets	$\mu+\geq 4$ jets
$t\bar{t} \rightarrow \ell$ +jets	59.0	56.3	37.1	39.4
$t\bar{t} \rightarrow \ell\ell'$	11.1	2.3	8.3	1.7
$W$ +jets	72.3 $\pm$ 11.6	10.7 $\pm$ 1.8	71.6 $\pm$ 10.7	14.9 $\pm$ 2.3
1 $b$ -tag multijet	21.8 $\pm$ 6.6	6.2 $\pm$ 2.8	5.8 $\pm$ 1.9	1.3 $\pm$ 1.0
others	4.5	1.1	3.2	0.9
background	98.6 $\pm$ 13.4	18.0 $\pm$ 3.4	80.6 $\pm$ 10.9	17.1 $\pm$ 2.5
data	172	88	135	92
$t\bar{t} \rightarrow \ell$ +jets	21.4	27.8	14.4	20.7
$t\bar{t} \rightarrow \ell\ell'$	4.8	1.1	3.7	0.8
$W$ +jets	5.7 $\pm$ 1.4	1.0 $\pm$ 0.3	6.0 $\pm$ 1.3	1.5 $\pm$ 0.4
$\geq 2b$ -tags multijet	3.0 $\pm$ 1.8	0.7 $\pm$ 0.9	0.8 $\pm$ 0.6	-0.1 $\pm$ 0.1
others	1.0	0.3	0.8	0.3
background	9.7 $\pm$ 2.3	2.0 $\pm$ 0.9	7.6 $\pm$ 1.5	1.7 $\pm$ 0.4
data	41	26	36	30

section. The measured cross section is the value of  $\sigma_{t\bar{t}}$  that maximizes  $\mathcal{L}$ . The details of this procedure can be found in Ref. [13] except that we do not use the nuisance parameter method for the systematic errors here.

## X. RESULTS

For a top quark mass of 175 GeV, we measure the  $t\bar{t}$  production cross-sections in the  $e$ +jets and  $\mu$ +jets channels

$$\begin{aligned}
 e + \text{jets} : \quad & \sigma_{p\bar{p} \rightarrow t\bar{t}+X} = 7.4 \pm 0.7(\text{stat})^{+0.8}_{-1.0}(\text{syst}) \pm 0.4(\text{lumi}) \text{ pb} \\
 \mu + \text{jets} : \quad & \sigma_{p\bar{p} \rightarrow t\bar{t}+X} = 9.5 \pm 0.9(\text{stat})^{+1.1}_{-1.3}(\text{syst}) \pm 0.6(\text{lumi}) \text{ pb}
 \end{aligned}$$

Both channels combined give

$$\ell + \text{jets} : \quad \sigma_{p\bar{p} \rightarrow t\bar{t}+X} = 8.3^{+0.6}_{-0.5}(\text{stat})^{+0.9}_{-1.0}(\text{syst}) \pm 0.5(\text{lumi}) \text{ pb}$$

in good agreement with theoretical predictions. In this combination we take the correlations between the  $e$ +jets and  $\mu$ +jets channels into account. The measured cross section depends somewhat on the assumed top quark mass. At 175 GeV the dependence is given by  $d\sigma/dm = -0.07$  pb/GeV.

Table 4 summarizes the systematic uncertainties. The largest systematic uncertainty arises from the  $W$ +heavy flavor fraction in the  $W$ +jets background model. The systematic uncertainty from the uncertainty in the integrated luminosity is 6.5% and quoted separately as the third uncertainty in the results.

TABLE 4: Summary of the systematic uncertainties in the top-antitop quark pair production cross section in pb.

source	$e$ +jets	$\mu$ +jets	combination
primary vertex	$\pm 0.13$	+0.16/ - 0.17	+0.14/ - 0.14
lepton ID	+0.33/ - 0.40	+0.63/ - 0.71	+0.34/ - 0.36
jet energy scale	+0.34/ - 0.45	+0.26/ - 0.43	+0.31/ - 0.44
jet id	$\pm 0.12$	$\pm 0.13$	$\pm 0.12$
jet resolution	+0.08/ - 0.09	+0.08/ - 0.09	+0.08/ - 0.09
trigger efficiencies	+0.04/ - 0.08	+0.22/ - 0.25	+0.09/ - 0.11
multijet background	$\pm 0.01$	$\pm 0.10$	$\pm 0.10$
$W$ +jets model	$\pm 0.45$	+0.52/ - 0.63	+0.48/ - 0.58
$b$ -tagging	+0.41/ - 0.44	+0.51/ - 0.55	+0.46/ - 0.49
other	+0.14/ - 0.15	+0.19/ - 0.20	$\pm 0.16$
total	+0.8/ - 1.0	+1.1/ - 1.3	+0.9/ - 1.0

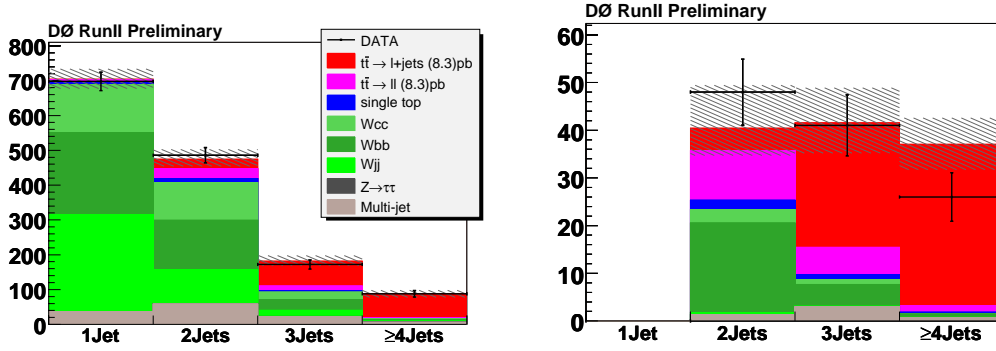


FIG. 3: The predicted sample composition for the  $e$ +jets samples with exactly one tagged jet (left) and with two or more tagged jets (right). The  $t\bar{t}$  contribution assumes the measured cross section value of 8.3 pb. The hatched band indicates the uncertainties in the model.

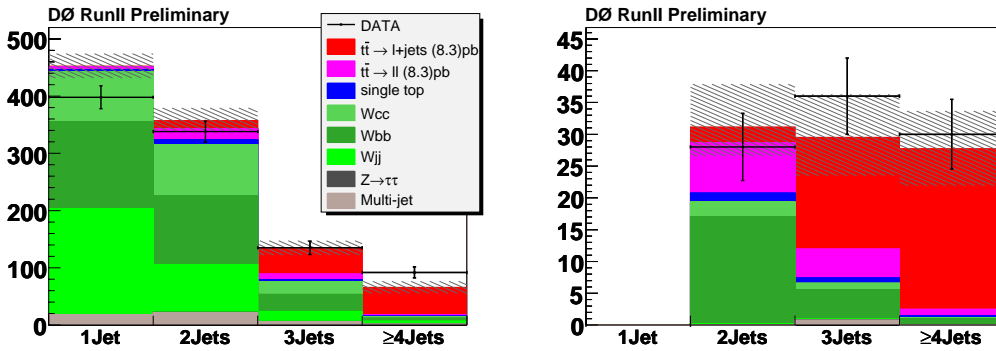


FIG. 4: The predicted sample composition for the  $\mu$ +jets samples with exactly one tagged jet (left) and with two or more tagged jets (right). The  $t\bar{t}$  contribution assumes the measured cross section value of 8.3 pb. The hatched band indicates the uncertainties in the model.

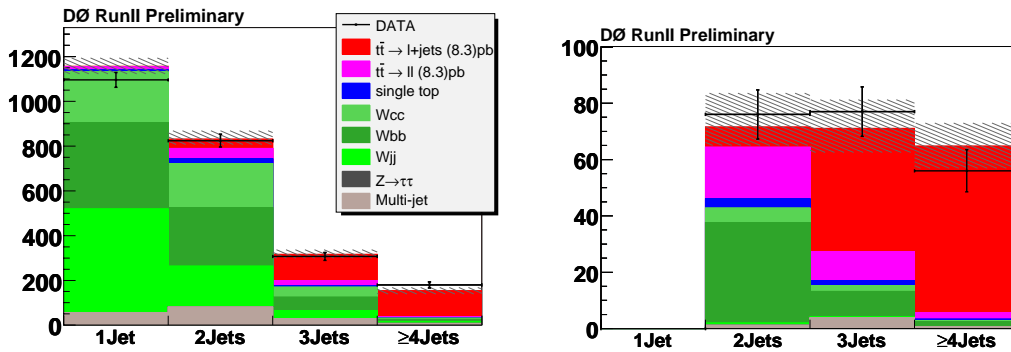


FIG. 5: The predicted sample composition for the the combined lepton+jets sample with exactly one tagged jet (left) and with two or more tagged jets (right). The  $t\bar{t}$  contribution assumes the measured cross section value of 8.3 pb. The hatched band indicates the uncertainties in the model.

#### Acknowledgements

We thank the staffs at Fermilab and collaborating institutions, and acknowledge support from the DOE and NSF (USA); CEA and CNRS/IN2P3 (France); FASI, Rosatom and RFBR (Russia); CAPES, CNPq, FAPERJ, FAPESP



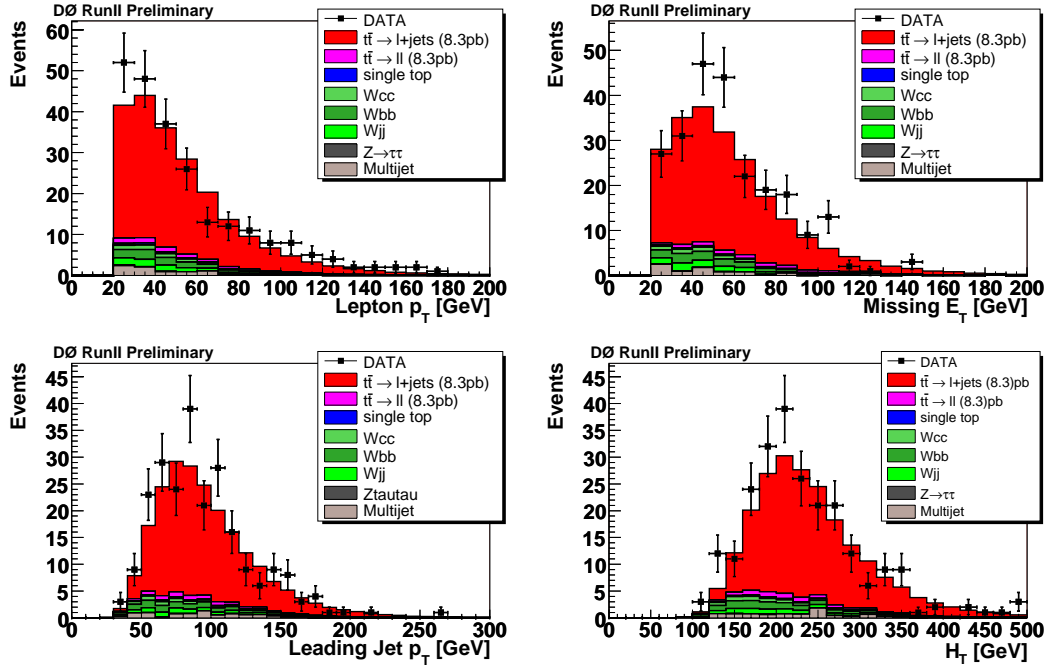


FIG. 6: The predicted sample composition for the lepton+jets samples with four or more jets for various kinematic variables. In these plots the measured  $t\bar{t}$  cross section of 8.3 pb was assumed.

and FUNDUNESP (Brazil); DAE and DST (India); Colciencias (Colombia); CONACyT (Mexico); KRF and KOSEF (Korea); CONICET and UBACyT (Argentina); FOM (The Netherlands); PPARC (United Kingdom); MSMT (Czech Republic); CRC Program, CFI, NSERC and WestGrid Project (Canada); BMBF and DFG (Germany); SFI (Ireland); The Swedish Research Council (Sweden); Research Corporation; Alexander von Humboldt Foundation; and the Marie Curie Program.

- 
- [1] N. Kidonakis and R. Vogt, “Next-to-Next-to-Leading Order Soft Gluon Corrections in Top Quark Hadroproduction,” Phys. Rev. D **68**,114014 (2003).
  - [2] M. Cacciari, S. Frixione, G. Ridolfi, M. Mangano, P. Nason, “The  $t\bar{t}$  Cross Section at 1.8 TeV and 1.96 TeV: A Study of the Systematics Due to Parton Densities and Scale Dependence”, JHEP **404**, 068 (2004).
  - [3] D0 Collaboration, V.M. Abazov *et al.*, Nucl. Instrum. and Methods A **565**, 463 (2006).
  - [4] D0 Collaboration, S. Abachi *et al.*, Nucl. Instrum. Methods Phys. Res. A **338**, 185 (1994).
  - [5] M. L. Mangano *et al.*, *ALPGEN, a Generator for Hard Multiparton Processes in Hadronic Collisions*, CERN-TH-2002-129, FTN-T-2002-06, hep-ph/0206293 (2002).
  - [6] T. Sjöstrand, L. Lönnblad, S. Mrenna, P. Skands, *PYTHIA 6.3: PHYSICS AND MANUAL*, LU-TP-03-38, hep-ph/0308153 (2003).
  - [7] S. Höche *et al.*, “Matching Parton Showers and Matrix Elements,” hep-ph/0602031.
  - [8] E.E. Boos *et al.*, “Method for Simulating Electroweak Top-Quark Production Events in the NLO Approximation: SingleTop Generator,” Phys. Atom. Nucl. **69**, 1317 (2006).
  - [9] S. Jadach, Z. Was, R. Decker and J. H. Kuhn, *The tau decay library TAUOLA: version 2.4*, Comput. Phys. Commun. **76**, 361 (1993).
  - [10] D. Lange, A. Ryd *et al.*, *The EvtGen Event Generator Package*, in Proceedings of CHEP (1998).
  - [11] S. Agostinelli *et al.*, Nucl. Inst. Meth. A506, 250 (2003).
  - [12] G. Blazey *et al.*, “Run II Jet Physics”, hep-ex/0005012.
  - [13] D0 Collaboration, V. M. Abazov *et al.*, Phys. Rev. D **74**, 112004 (2006).